Available online at www.sciencedirect.com
ScienceDirect
Journal of Pharmaceutical and Biomedical Analysis 45 (2007) 572–582
JOURNAL OF PHARMACEUTICAL AND BIOMEDICAL ANALYSIS
www.elsevier.com/locate/jpba

Chromatographic analysis and decomposition product characterization of compound SR16157 (NSC 732011)

Jennie Wang [a,*], ChunYang [a], Euphemia Wang [a], Shihong Li [a], Nurulain Zaveri [a], Paul Liu [b]

[a] *SRI International, 333 Ravenswood Ave, Menlo Park, CA 94025, USA*
[b] *Pharmaceutical Resources Branch, DCTD, NCI, 6130 Executive Blvd., Bethesda, MD 20892, USA*

Received 18 April 2007; received in revised form 21 July 2007; accepted 2 August 2007
Available online 19 August 2007

Abstract

SR16157 (21-(2-*N*,*N*-diethylaminoethyl)oxy-7α-methyl-19-norpregna-1,3,5(10)-triene-3-*O*-sulfamate) is a novel, dual-acting estrone sulfatase inhibitor currently in preclinical development for use in breast cancer therapy. The compound has a dual mechanism of action: the sulfamate-containing parent compound SR16157 inhibits estrogen biosynthesis by irreversibly inhibiting the enzyme estrone sulfatase. The phenolic metabolite, SR16137, generated by the sulfatase enzyme is a potent antiestrogen in breast tissues and has beneficial effects in bone and the cardiovascular system.

As part of the ongoing preclinical studies, an HPLC assay method has been developed and validated for SR16157. The assay method is specific, accurate (recovery = 99.4–101.1), linear ($r^2 \geq 0.9999$), precise (intraday R.S.D. ≤ 1.1%, intermediate R.S.D. ≤ 0.8%), and sensitive (limit of detection = 1.0 μg/ml). It separates SR16157 from its impurities and forced decomposition products, which have been characterized by LC coupled with mass and UV spectral data. Major decomposition pathways are hydrolysis, hydroxylation, and oxidation.

Keywords: SR16157; NSC 732011; Forced decomposition; HPLC assay; Validation; Impurity characterization

1. Introduction

Two-thirds of breast cancer cases occur in postmenopausal women, and about 50% of them are estrogen dependent. In postmenopausal women, estrogens are synthesized from circulating inactive precursors and exert their mitogenic effects on tumor growth by their action at the estrogen receptor. Endocrine (antihormonal) therapy is the mainstay of therapy for estrogen-dependent breast cancer. Two general approaches have been clinically validated for endocrine therapy of breast cancers: (i) antagonism of estrogen action at the estrogen receptor (antiestrogens) and (ii) inhibition of estrogen biosynthesis. Estrogen receptor antagonism with selective estrogen receptor modulators (SERMs) such as tamoxifen has been successfully used for breast cancer therapy for over three decades. Estrogen biosynthesis, on the other hand, is dependent on three enzymes: aromatase, estrone sulfatase, and 17β-hydroxysteroid dehydrogenase. Aromatase inhibitors are now being used as first-line therapy for estrogen-dependent breast cancer. The enzyme estrone sulfatase (also called steroid sulfatase, STS) also plays a major role in the production of active estrogen from inactive precursors in tumor tissue (Fig. 1). In postmenopausal women, circulating plasma estrogen is present mainly in the inactive sulfated form, and is converted to active estrogen by the action of steroid sulfatase in breast and other peripheral tissue [1]. In breast tissue, steroid sulfatase contributes to 10-fold higher production of estrogen than the aromatase enzyme [2,3]. STS activity is found to be up to 200 times higher than aromatase activity [4] in breast tumor tissue. Furthermore, higher levels of STS mRNA are found in malignant compared to normal breast tissue and are associated with poor prognosis [5]. Therefore, STS is a good target for inhibition of estrogen biosynthesis and represents a new approach for the endocrine therapy of breast cancer. Although several STS inhibitors have been reported in literature [6], only one compound, 667 COUMATE, has advanced to Phase I clinical trials in the United Kingdom [7].

* Corresponding author. Fax: +1 650 859 2753.
E-mail address: jennie.wang@sri.com (J. Wang).

0731-7085/$ – see front matter © 2007 Elsevier B.V. All rights reserved.
doi:10.1016/j.jpba.2007.08.015

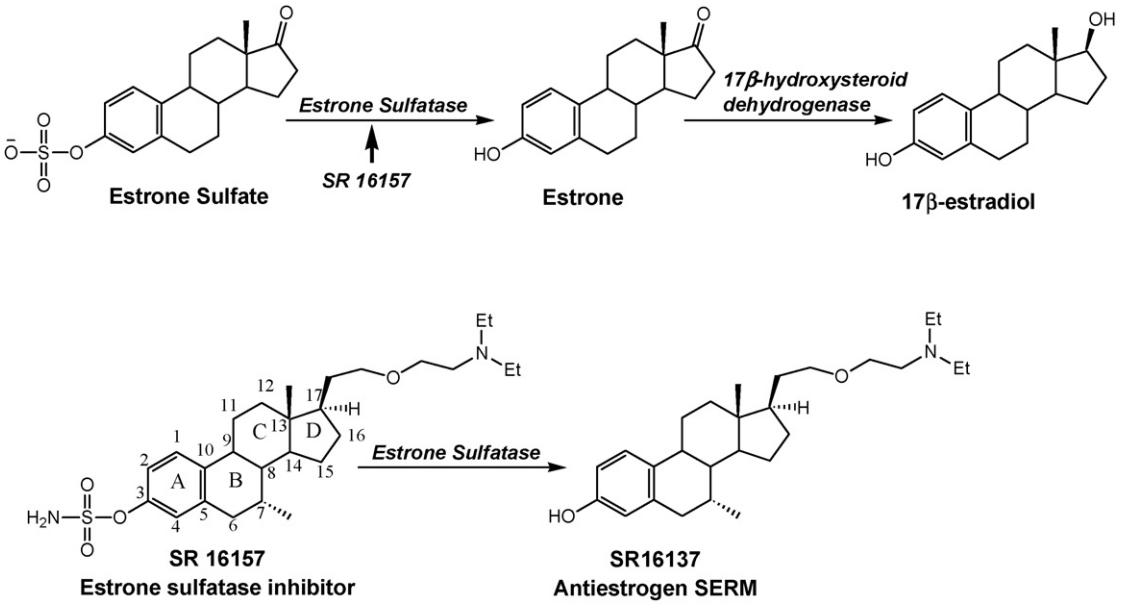

Fig. 1. Enyzmatic conversion of estrone sulfate to estrone and estradiol, and the conversion of sulfamate-based sulfatase inhibitor SR16157 to the antiestrogen SERM SR16137.

We have discovered a novel and potent estrone sulfatase inhibitor, SR16157, which is currently in late-stage preclinical development [8]. SR16157 is a sulfamate-containing steroidal compound with a unique, dual-targeted mechanism of action. The parent sulfamate SR16157 (21-(2-*N*,*N*-diethylaminoethyl)oxy-7α-methyl-19-norpregna-1,3,5(10)-triene-3-*O*-sulfamate) is a potent, irreversible inhibitor of estrone sulfatase. It is transformed by estrone sulfatase to a novel phenolic steroidal SERM, SR16137 (Fig. 1), and therefore potentially offers a dual mechanism for inhibition of estrogenic action via inhibition of estrogen biosynthesis and estrogen receptor antagonism [9].

The compound is in preclinical development, supported by the National Cancer Institute's (NCI's) Rapid Access to Intervention Development (RAID) program. As part of this preclinical development, we have performed detailed chemical and chromatographic analysis of this steroidal compound. We report here a reversed-phase HPLC assay method, along with characterization of decomposition products for SR16157. The assay method has been validated for specificity, accuracy, precision, linearity, and sensitivity. Identities of impurities and forced decomposition products of SR16157 were elucidated by their mass and UV spectral data. The analytical method will be useful in characterization of the drug substance and drug product. Information on degradation pathways and degradation conditions, as well as on identities of degradation products, will be useful for future formulation and metabolic pathway studies.

2. Experimental

2.1. Chemicals and reagents

SR16157 (NSC 732011) was provided by the NCI (Bethesda, MD, USA). SR16137 was synthesized in house at SRI International (Menlo Park, CA, USA). Anhydrous trifluoroacetic acid (TFA), estrone (E1), 4-hydroxylestrone (4-OH E1), and 16α-hydroxylestrone (16α-OH E1) were purchased from Sigma Chemical (St. Louis, MO, USA). 2-hydroxylestrone (2-OH E1) was purchased from Fisher Scientific (Pittsburgh, PA). HPLC grade acetonitrile (ACN) and hydrogen peroxide (H_2O_2) 30% solution were purchased from Mallinckrodt (Paris, KY, USA). Water was purified through a Millipore Super-Q Pure Water System (Waltham, MA, USA). Solutions of HCl and NaOH were prepared from Dilute-it Analytical Concentrate (J.T. Baker, Phillipsburg, NJ, USA).

2.2. HPLC

A Hewlett-Packard 1050 HPLC system (Wilmington, DE) equipped with a solvent degasser, pump, autosampler, and variable wavelength UV detector was used in the study. A 1040 photo diode-array (PDA) detector was employed for peak purity analysis. HP ChemStation® for LC (A 05.02) software was used for instrument operation control and data collection. In the method validation of intermediate precision, a second HPLC system, the Agilent 1100 system, was used. The HPLC was performed on a Phenomenex Luna C18 (2) column (5 μm, 250 mm × 4.6 mm i.d., Torrance, CA, USA). The column was held at 27 °C. The mobile phase was a combination of solvent A (0.1% TFA in water) and solvent B (0.08% TFA in ACN). For assay, an isocratic elution at 45% of solvent B and 55% of solvent A was used. The injection volume was 5 μl. For qualitative analysis and investigation of decomposition products, the following gradient program was used: 0–20 min, 45% solvent B and 55% solvent A; 20–39 min, linear gradient to 95% solvent B and 5% solvent A; 39–44 min, hold at 95% solvent B and 5% solvent A; 44–52 min, re-equilibrate at 45% solvent B and 55% solvent A before the next injection. The injection volume was

10 μl. For both isocratic and gradient conditions, the elution flow rate was 1.0 ml/min, and the detection wavelength was set at 220 nm.

LC–MS was performed on a ThermoQuest system consisting of a Surveyor LC pump, a Surveyor autosampler, a Surveyor PDA UV detector, and a Finnigan LCQ-DUO ion trap mass spectrometer (San Jose, CA, USA). The PDA UV detector was used for recording UV–visible spectra. The mass spectrometer was equipped with an electrospray ionization (ESI) probe operating at atmospheric pressure. The ESI source parameter settings were: spray voltage 5 kV; capillary voltage 33 V; capillary temperature 250 °C; tube lens offset 0 V; sheath gas flow rate 80 units; auxiliary gas flow rate 20 units. Tandem mass spectrometry was performed at 85% normalized collision energy level. Signals with mass range of *m/z* 150–800 were collected. The LC conditions used for identification of decomposition products of SR16157 were the same as those described above except that the elution was isocratic at 55% solvent A and 45% solvent B with a flow rate of 0.5 ml/min. Matching of the peak identity between the LC-UV system (Hewlett Packard 1050) and LC–MS system (ThermoQuest) was achieved by relative retention time and relative UV peak intensity. Each forced degradation solution was divided into two portions and analyzed by both systems on the same day to ensure comparable peak intensities.

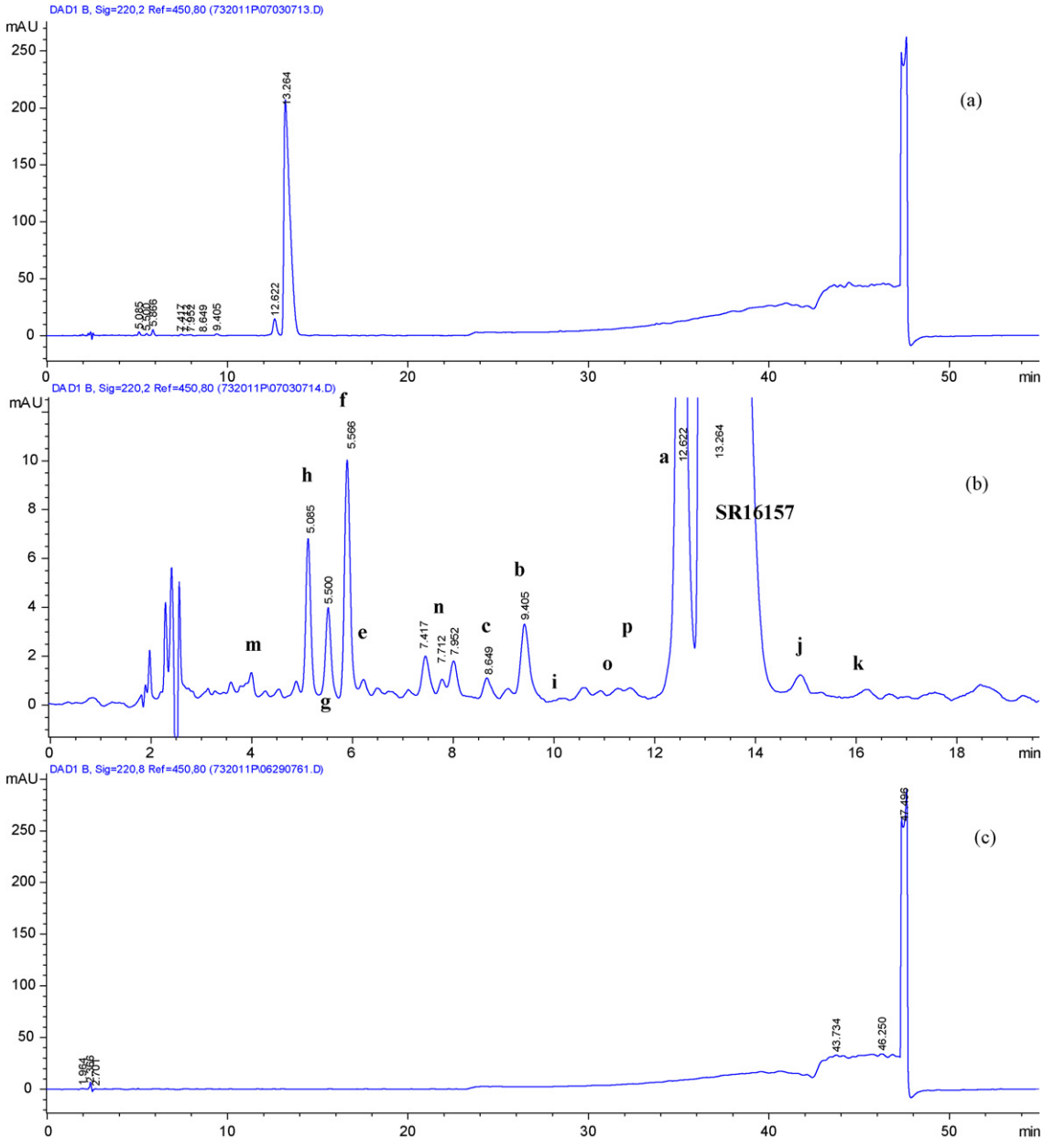

Fig. 2. Chromatograms of thermally stressed SR16157 (solution E) and a solvent blank injection. (a) Thermally stressed, full scale. (b) Thermally stressed, expanded scale. (c) Solvent blank injection.

Table 1
Preparation of the forced decomposition solution

Solution ID	Preparation
A	0.5 ml of the stock solution was mixed with 0.5 ml of 0.1% TFA in ACN/H_2O (1:1)
B	0.5 ml of the stock solution was mixed with 0.5 ml of 0.01N HCl, heated at 60 °C for 1 h and neutralized with 0.5 ml of 0.01N NaOH before injection
C	0.5 ml of the stock solution was mixed with 0.5 ml of 0.025N NaOH, allowed to stand at room temperature for 2 h and neutralized with 0.5 ml of 0.025N HCl before injection
D	0.5 ml of the stock solution was mixed with 0.5 ml of 5% H_2O_2 and heated at 60 °C for 1 h
E	1 mg of the solid sample was heated in a heating block at 80 °C for 11 days, and then dissolved in 2 ml 0.1% TFA in ACN/H_2O (1:1)
F	1 mg each of the solid sample was placed into two individual clear glass vials, one wrapped with foil as control and the other unwrapped. These two vials were stored in the environmental chamber with both UV-A light and cool white light on for 30 h and then the cool white light on for an additional 120 h. They were finally dissolved in 2 ml of 0.1% TFA in ACN/H_2O (1:1)

2.3. Environmental chamber for photo stressed decomposition

The forced degradation study under UV and visible light was carried out in the ES 2000 Environmental Chamber (Environmental Specialties, Inc., Raleigh, NC, USA), equipped with a cool white lamp (8.0 kilolux) and a UV-A lamp (14.00 W/m^2), in conformance with the ICH Q1B option 2 for photostability testing. Temperature and humidity conditions were set at 25 °C/60% RH.

2.4. Sample preparation

2.4.1. Forced decomposition sample solutions

A stock solution of 0.5 mg/ml SR16157 in ACN/H_2O (1:1) with 0.1% TFA was prepared. Forced decomposition samples under various stressed conditions were prepared from the stock solution as described in Table 1.

2.4.2. For validation of linearity, accuracy and precision

Accurately weighed 0.1–1.5 mg portions of SR16157 were dissolved in 2.0 ml of ACN/H_2O (1:1) with 0.1% TFA to yield solutions at 0.05, 0.1, 0.25, 0.5, 0.63, and 0.75 mg/ml. The solutions were sonicated to ensure complete dissolution.

3. Results and discussion

3.1. HPLC method development

Reversed-phase HPLC (RP-HPLC) is commonly used in steroid hormone drug analyses. As described in Görög's review article [10], it is the predominant method in the United States Pharmacopoeia for assay and related impurities tests

Table 2
Summary of the observed peaks

t_R (min)	RRT[a]	*m/z*	λ_{max} (nm)	Possible identity	Comment/significant changes
3.2	0.24				imp.[b]
3.5	0.26				imp.
3.9	0.29	430	230, 280	**m**	imp., increased in HCl heated, NaOH, and thermal
4.4	0.33	509	215, 260	**h′**	imp.
4.8	0.36	509	225, 265	**h**	imp.
5.1	0.38	507	225	**e′**	increased in HCl
5.5	0.41	428	225, 255, 325	**g**	imp., increased in HCl heated, NaOH, thermal
5.7	0.43	525	220, 265	**d**	generated in H_2O_2 and UV
5.9	0.44	572	225, 270	**f**	imp.
6.4	0.48	507	250, 295	**e**	imp., increased thermal, decreased in HCl heated
7.3	0.55				imp.
7.9	0.59	651	225, 270	**n**	imp., decreased in HCl heated and H_2O_2
8.6	0.65	386	225, 280	**c**	generated in HCl heated and NaOH
8.7	0.65				imp.
9.4	0.71	465	225, 265	**b**	generated in HCl, H_2O_2, thermal, and UV
9.7	0.73	523	235, 290	**I**	generated in thermal
10.4	0.78				imp.
11.2	0.84	412	265, 300	**o**	imp., increased in NaOH
11.8	0.89	491		**p**	imp.
12.6	0.95	414	225, 280	**a**	imp., increased in all stressed solutions
13.3	1.00	493	225, 275	SR16157	NSC 732011
14.9	1.12	507		**j**	imp.
15.8	1.19	430		**m′**	generated in HCl and NaOH
16.3	1.23	509	220, 275	**k**	imp.
27.2	2.14				imp.
28.5	2.27				imp.
30.2	0.24				imp.

[a] RRT: t_R/t_R major peak.
[b] imp.: Sample impurity.

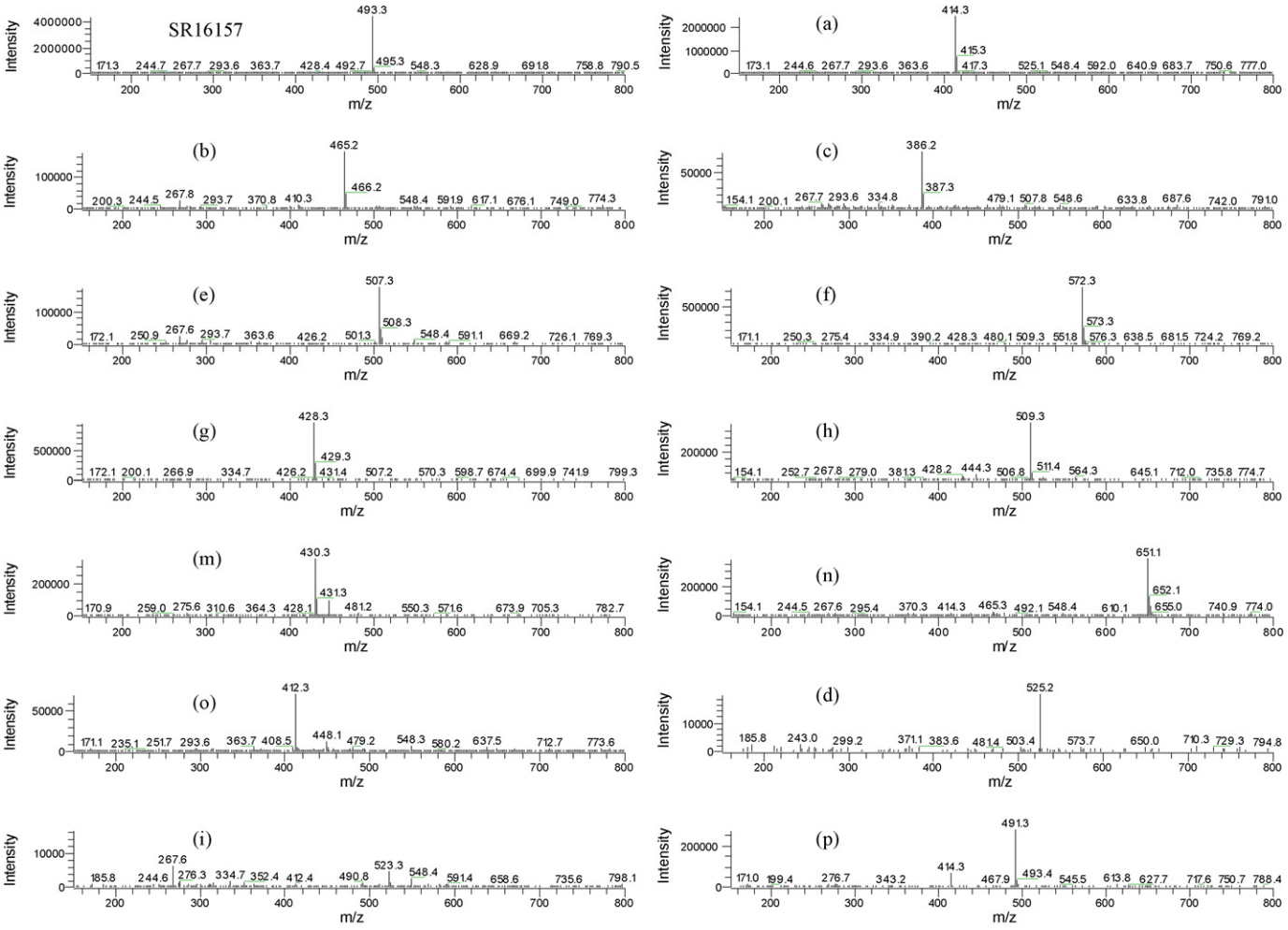

Fig. 3. Mass spectra of SR16157 and products **a**–**i**, **m**–**p**.

of bulk steroid hormones and hormone-like structures. In the overwhelming majority of cases, porous octadecylsilica support (3–10 μm) is used for the reversed-phase separations. Unbuffered binary or ternary mixtures of water with methanol, acetonitrile, or tetrahydrofuran are used as the mobile phase. For steroids that possess ionizable groups, the aqueous phase in some cases contains phosphate buffer, acetic acid, or ion pair reagents [11]. The applicability of the RP-HPLC separation in estrogen-related compounds was demonstrated by the work of Nygaard et al. in which 10 impurities and degradation products were resolved from the active drug 17β-estradiol using a Waters Symmetry C18 column and water–ACN mobile phase [12].

Since RP-HPLC is most commonly used for the analysis of estrogens, the effort to develop a method for SR16157 was initiated with C18 and C8 columns. The following columns were tested: Eclipse XDB C8 (5 μm, 150 mm × 4.6 mm i.d., Agilent Technology, Wilmington, DE, USA), Ace C18 (3 μm, 150 mm × 4.6 mm i.d., Mac-Mod Analytical, Chadds Ford, PA, USA) and Luna C18 (2) (5 μm, 150 mm × 4.6 mm and 250 mm × 4.6 mm i.d., Phenomenex, Torrance, CA, USA). The mobile phase was a combination of ACN and water. With the ACN content at 40–50%, the compound has a reasonable retention time ($k' = 4$–5) on the above-listed columns. TFA was added to the mobile phase to suppress the reactivity of the residual silanol and curtail tailing. Among the columns tested, the Luna C18 (2) (5 μm, 250 mm × 4.6 mm i.d.) provided the best separation between impurities closely eluting with SR16157 (i.e., impurities **a** and **j**; see Fig. 2) and the most symmetrical peak shape. Thus the Luna C18 column was chosen for further refinement of the composition of the mobile phase. Before the method was finalized, a complete gradient program, 5–95% ACN in 30 min, was used to detect possible early or late eluting decomposition products. No significant early or late eluting components were found. For separation of impurities **a** and **j**, the optimal mobile phase composition was found to be 45% ACN and 55% water, each containing 0.08% and 0.1% TFA, respectively. As assurance for the completeness of the impurity profile, a gradient from 45% to 95% ACN in 19 min was added. Three trace impurities were observed in the gradient portion of the elution (Table 2). To minimize the baseline drift in the gradient elution, the TFA content was made unequal, with 0.08% in ACN and 0.1% in water, to correct for the varying UV absorptivity.

In order to obtain a decomposition profile that closely simulates stability testing conditions, forced degradation was targeted at a level which is equal to 5–20% decrease of the active drug, as recommended in literature [13]. The conditions that led to the

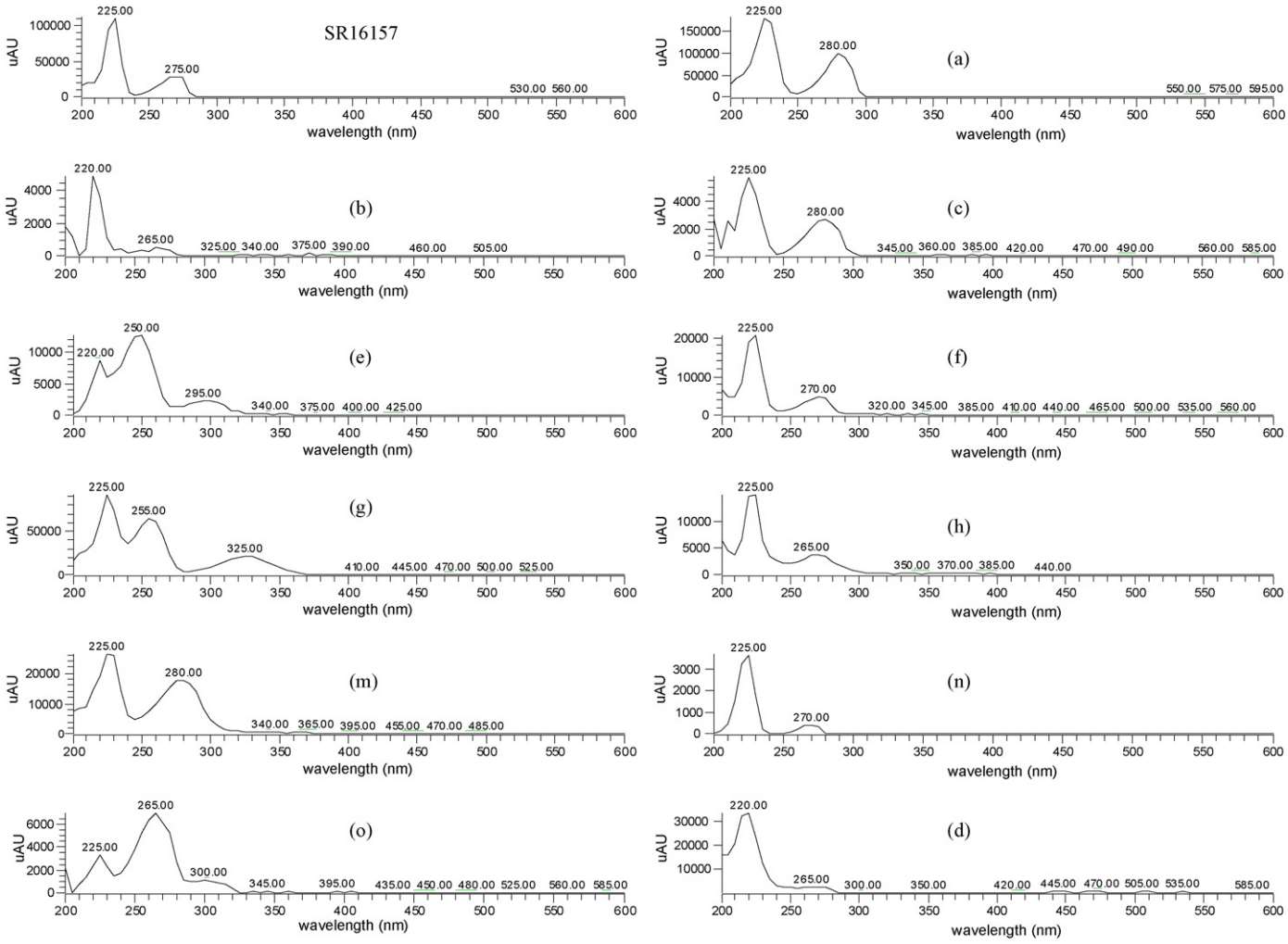

Fig. 4. UV spectra of SR16157 and products **a**–**h**, **m**–**o**.

targeted decrease were found after several trial runs, as presented in Table 1. The optimized LC condition separated SR16157 from all decomposition products. Additionally, major decomposition products are adequately resolved from one another. A representative chromatogram, from the heated solid sample, and a chromatogram of the solvent blank are shown in Fig. 2. The peak of SR16157 in all forced decomposition sample chromatograms passed the peak purity check performed by the HP ChemStation® software. When examined by LC/MS, no impurity was found within the peak of SR16157 in any forced decomposition sample chromatogram. These findings indicate that the method is specific for analysis of SR16157. Mass balance was assessed by comparing the decrease in SR16157 and the increase in all detectable degradants. The total peak area in each forced decomposition sample was not less than 93% of that before decomposition. As the major decomposition product is **a**, which is identified as compound SR16137 (see Section 3.2), the UV molar extinction coefficients ε of SR16157 and SR16137 were measured and found to be 9000 and 8000 $cm^{-1}\,l\,mol^{-1}$, respectively, at the HPLC detection wavelength of 220 nm. With consideration of the difference in UV absorptivity, the decrease in SR16157 was mostly (>94%) accounted for by the corresponding increase in product **a** (SR16137) in all the decomposition solutions. A reasonable mass balance was achieved.

It is noteworthy that SR16157 is susceptible to base-catalyzed hydrolysis. Dissolving the compound in 0.1N NaOH led to an instant decrease of the main peak to 75%. Over time, the compound decreased to 10% (in 45 min) and 2% (in 12 h). A concomitant increase in the peak area of the hydrolysis product **a** was recorded, along with increases in other minor decomposition products, e.g., the hydroxylation product **m** (*m*/*z* 430) and the corresponding oxidation product **g** (*m*/*z* 428) (see Section 3.2).

3.2. Characterization of decomposition products

Table 2 lists the observed peaks from all the forced degradation solutions. Representative mass and UV spectra of impurities and degradation products obtained through LC with MS and PDA detections are shown in Figs. 3 and 4. The observed molecular ions and wavelengths of maximum UV absorption (λ_{max}) of these compounds are also listed in Table 2. An alphabetic letter was assigned to the components for which MS and UV data

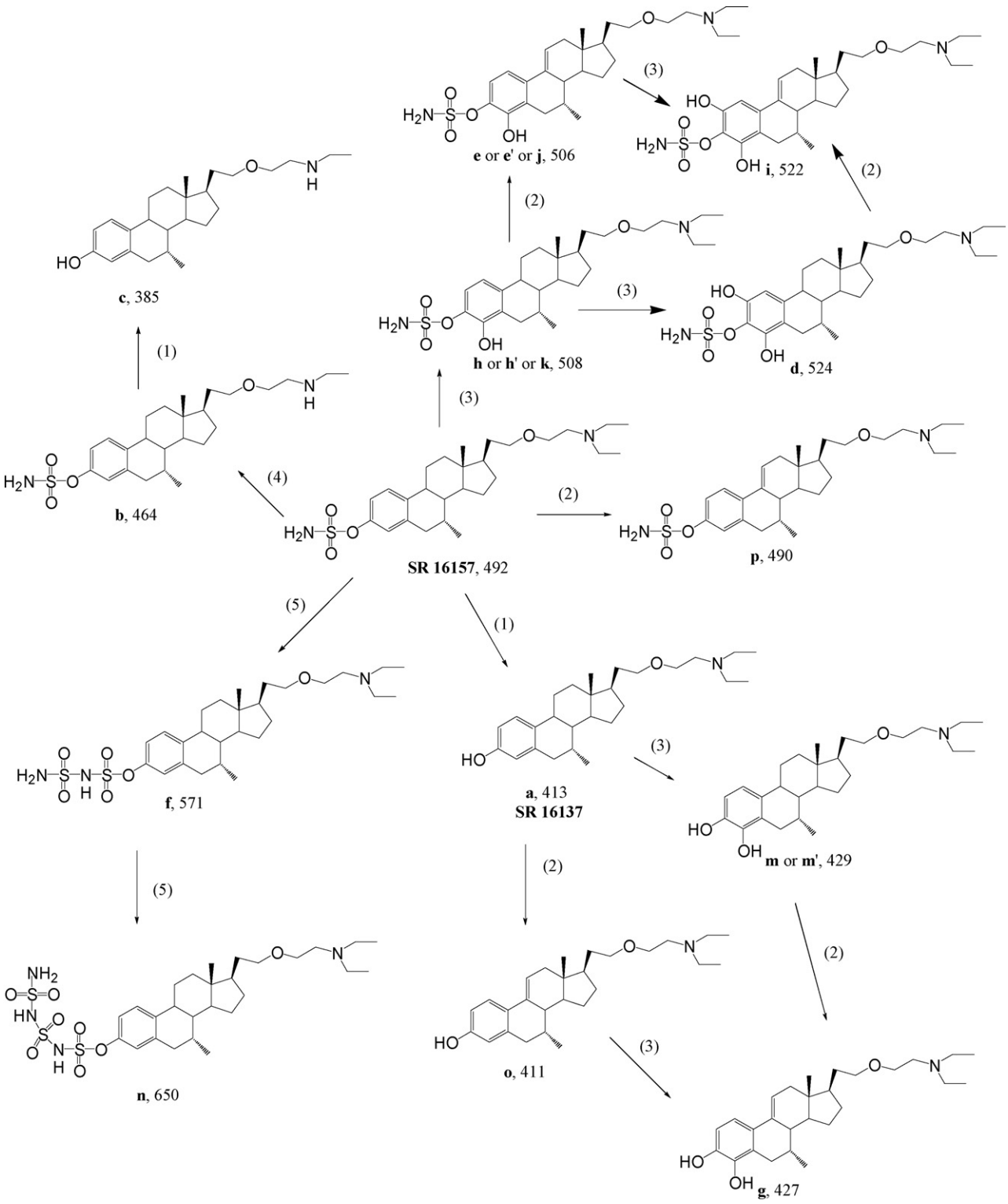

Fig. 5. Proposed structures of impurities and decomposition products formed via pathways as indicated on the arrows: (1) hydrolysis of the sulfamate; (2) oxidation; (3) hydroxylation; (4) de-ethylation; (5) side reaction in the synthesis process. The numbers next to the structure identification letters show the molecular weight of the respective components.

are available. Possible identities of these impurities are deduced from spectral (MS and UV) data as well as mechanistic considerations. The process of generating all the observed impurities can be classified as follows: (1) hydrolysis of the sulfamate; (2) oxidation; (3) hydroxylation; (4) de-ethylation; and (5) side reaction in the synthetic process. The proposed structures are presented in Fig. 5.

The most significant degradant is the hydrolysis product **a**. Its molecular ion is *m/z* 414 which is 79 mass units lower than that of the parent drug SR16157 (*m/z* 493). Since chemical reactivity

predicts that the sulfamate is the most labile functional group, it is straightforward to assume that product **a** is generated through hydrolysis of the sulfamate moiety (M−80+H), catalyzed by the nucleophilic hydroxyl ion. The identity of the resultant phenolic compound (SR16137; see Figs. 1 and 5 for its structure) is also confirmed by spiking the solutions of SR16157 with an authentic sample of SR16137. Co-elution of SR16137 and product **a** was observed. The UV spectral data of product **a** and SR16137 are identical. Analogously, the molecular ions of product **b** (*m/z* 465) and product **c** (*m/z* 386) differed by 79 mass units, indicating that **c** is the desulfamated **b**, where **b** is a de-ethylated product of SR16157 (28 mass units less, [M−CH_2CH_3+H]).

Among the observed impurities and decomposition products, companion compounds with differences of 2 mass units appeared frequently, including pairs with *m/z* 509/507 (**h/e**), 414/412 (**a/o**), 430/428 (**m/g**), 525/523 (**d/i**), and 493/491 (SR16157/**p**), as shown in Table 2. For those with available UV profiles (Fig. 4), the λ_{max} of the lower mass component always shifts to a longer wavelength (red shift), probably as a result of an extended conjugation formed by dehydrogenation (oxidation) of the respective high mass component in the pair. The double bond could be $\Delta^{6,7}$, $\Delta^{8,9}$, or $\Delta^{9,11}$, which would be expected to extend the conjugation in the A ring (see Fig. 1 for structural position labels). UV spectral data are well documented for the isomeric ($\Delta^{6,7}$, $\Delta^{8,9}$, and $\Delta^{9,11}$), unsaturated, steroidal phenols. As the quality of the UV spectra for the pair of 414/412 (**a** and **o**) is good (Fig. 4) and their chromophoric structures are closest to the example compounds found in the literature (i.e., 3-OH instead of 3-*O*-sulfamates or di-hydroxylated A ring), they are taken as the representative pair for structural-UV profile examination. Based on literature examples [14,15], the $\Delta^{8,9}$ isomer usually exhibits an absorption band at 274 nm and negligible absorbance around 300 nm. Because product **o** does not follow this pattern, the $\Delta^{8,9}$ structure can be ruled out for product **o**. The $\Delta^{6,7}$ and $\Delta^{9,11}$ isomers have absorption bands at 261–272 and 298–306 nm. The intensity ratios of the two bands would be 3:1 for the $\Delta^{6,7}$ isomer and 6:1 for the $\Delta^{9,11}$ isomer. Product **o** showed a 6:1 ratio of intensities of the two bands at 265 nm and 300 nm, and therefore it was concluded that product **o** is the $\Delta^{9,11}$ isomer. Although direct UV data for other unsaturated impurities and decomposition products (i.e., the 3-O-sulfamates or di-hydroxylated A ring) are not available, based on the proposed structure of product **o,** a reasonable assumption is that $\Delta^{9,11}$ forms more easily than $\Delta^{6,7}$ and $\Delta^{8,9}$. Therefore, those decomposition products (**e**, **e′**, **j**, **g**, **p**, and **i**) are also assumed to be $\Delta^{9,11}$ isomers, as shown in Fig. 5.

Hydroxylations at the 2, 4, and 16 positions are well-known metabolic pathways for estrogens [16–21]. In the case of SR16157, multiple sites of hydroxylation were observed because there were several products with *m/z* 509 (**h**, **h′**, and **k**), *m/z* 507 (**e**, **e′**, and **j**), and *m/z* 430 (**m** and **m′**). Component **m** is proposed to be the monohydroxylated product of **a**. UV spectra of **m** and **a** displayed similar absorption bands at 225 and 280 nm, respectively. The chromophoric structure of **a** is similar to that of estrone (E1). E1, 2-OH E1, 4-OH E1, and 16α-OH E1 are available as the model compounds for studying the hydroxylation position of **m**. The UV spectra of E1, 2-OH E1, 4-OH E1, and 16α-OH E1 in the same solvent mixture used in the mobile phase were obtained with a Diode Array Spectrophotometer (Hewlett-Packard 8452A). The results are shown in Fig. 6. The UV spectra of E1, 4-OH E1, and 16α-OH E1 have similar absorption bands at 280 nm, whereas 2-OH E1 displays a different absorption band at 288 nm. Analogously, 2-hydroxylated estradiol (2-OH E2) also exhibits an absorption maximum at 288 nm [22]. Based on the UV data shown in Fig. 4 (**m**, λ_{max} 280 nm), it is unlikely that **m** would have the hydroxyl substitution at C-2. Because of the scarcity of samples, further elucidation of the substitution pattern of the series of hydroxylated products (**e**, **e′**, **j**, **h**, **h′**, **k**, and **m** and **m′**) by NMR was not pursued. Based on chemical reactivity, C-4 and C-6 are expected preferentially to undergo hydroxylation. The C-4 hydroxylation pattern for these degradants, as depicted in Fig. 5, is arbitrary.

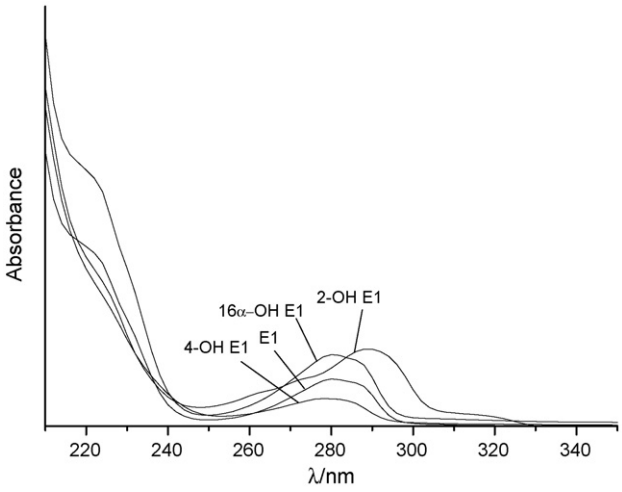

Fig. 6. UV spectra of E1, 2-OH E1, 4-OH E1, and 16α-OH E1 in a mixture of ACN/H_2O (V/V = 45:55) with 0.1% TFA.

Two impurities with molecular mass higher than that of the parent drug were detected in a few pilot synthesis lots. They were impurities **f** (*m/z* 572) and **n** (*m/z* 651). They are 79 mass units higher (for **f**) or twice 79 mass units higher (for **n**) than the parent drug (*m/z* 493). They are assumed to be the process-related, oversulfamated by-products, as depicted in Fig. 5. This assumption is plausible because of the known property of the sulfamic acid reagent, which reacts readily with OH or NH_2 to form O substituted or N substituted sulfamates.

To obtain further proof of the proposed structures of impurities and decomposition products, tandem mass spectrum (MS/MS) was attempted. Three common fragmentation patterns are observed. The first one is the loss of sulfamate, resulting in the M-80 fragment, presumably a positively charged radical ion, in products **j** (507 → 427), **k** (509 → 428), SR16157 (493 → 413), and **p** (491 → 411). The second pattern is the loss of the diethylamino ethanol ($HOC_2H_4N(C_2H_5)_2$, M-117), observed in product **o** (412 → 295). The third pattern is the fragment of *m/z* 173, probably resulting from the steroidal backbone AB rings, which was observed in the MS/MS spectra of products **a** and **c**. Typical MS/MS spectra are shown in Fig. 7. The MS/MS fragmentation was consistent with the proposed structures, although it did not explicitly confirm the

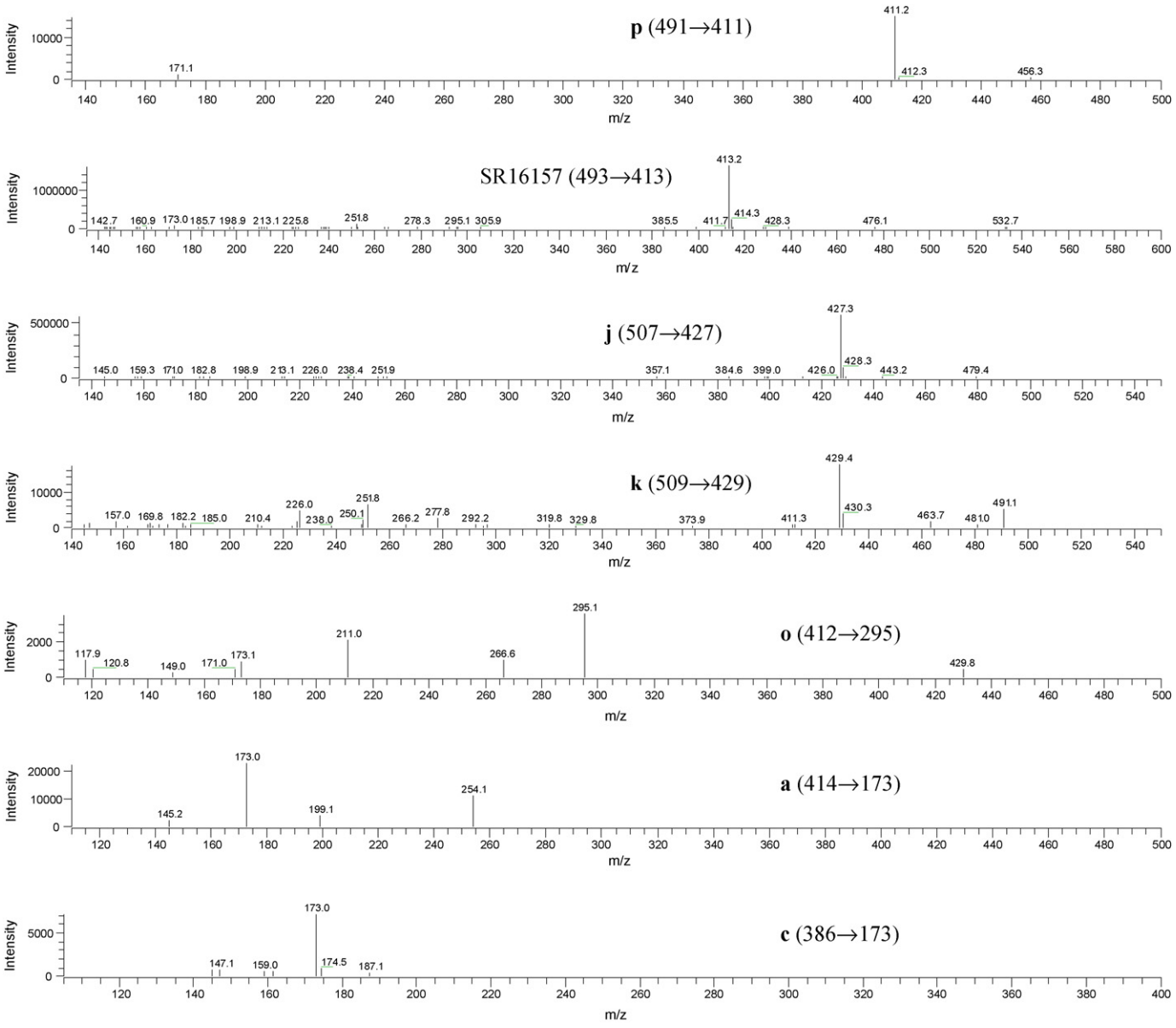

Fig. 7. Tandem mass spectra of **p**, SR 16157, **j**, **k**, **o**, **a**, and **c**.

hydroxylation, de-ethylation, and oxidation (dehydrogenation) products.

Overall, the most significant decomposition pathway is the hydrolysis of the sulfamate. The resulting product **a** is the phenolic compound (SR16137), a known estrogen antagonist [9]. Other proposed structures of the degradants will be confirmed in future studies by total synthesis and spectral investigation.

3.3. Validation of the HPLC assay

The proposed method was validated in accordance with the current ICH guideline Q2 (R1). Fig. 8 is a typical chromatogram of the HPLC assay. SR16157 elutes at 13.8 min. The results described in Section 3.1 have demonstrated the specificity of the method. The system suitability data are presented in Table 3.

Three sets of validation were designed by varying analysts, equipment, and days. Validation 1 and 2 were performed by a single analyst on one LC system (the Hewlett-Packard 1050 system) on two different days. Validation 3 was performed by a second analyst on a different LC system (the Agilent 1100 system).

Table 3
System suitability

Chemical	SR16157
Retention time (min)	13.8
Capacity factor, k'	4.7
Resolution to **a**	1.8
USP tailing factor	1.6
Number of theoretical plates/column	10,565
% R.S.D. in peak areas from six injections	0.23

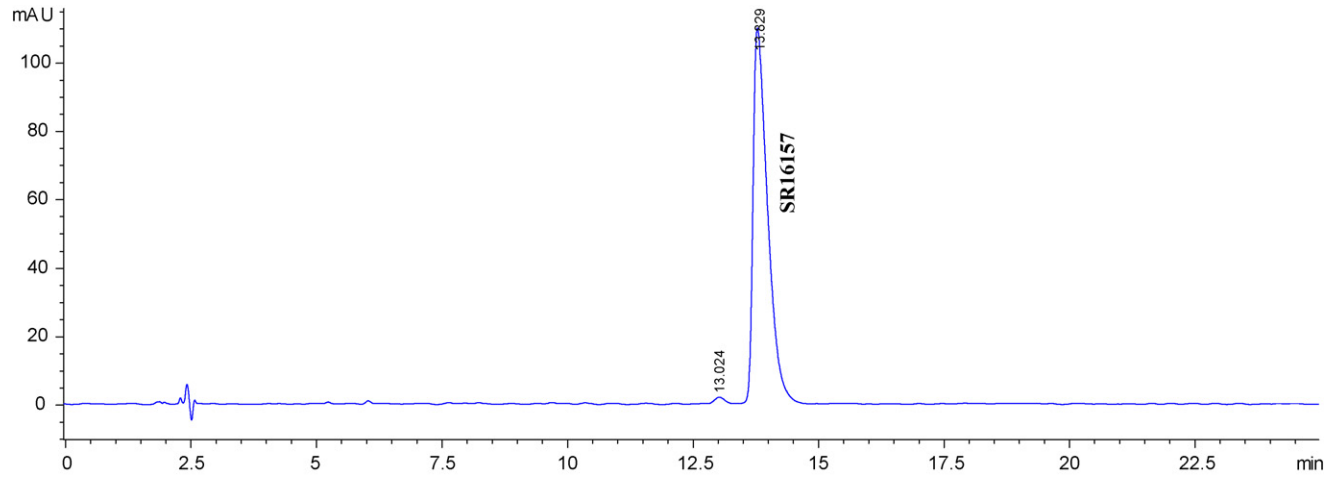

Fig. 8. A chromatogram of SR16157 assay.

Table 4
Linearity data on SR16157 standard curves

Standard curve	Slope	y-Intercept	r^2 value
Validation 1	4619.69	−4.34	1.0000
Validation 2	4548.74	1.78	0.9999
Validation 3	4812.24	−4.35	1.0000

Table 5
Accuracy: average percent recoveries of three preparations/determinations at each concentration

	0.05 mg/ml	0.5 mg/ml	0.75 mg/ml
Validation 1	101.08	100.45	100.29
Validation 2	100.95	99.87	100.82
Validation 3	100.00	99.44	99.88

Linearity of the method was demonstrated by standard curves for the range of 0.05–0.75 mg/ml. Six solutions at 0.05, 0.10, 0.25, 0.50, 0.63, and 0.75 mg/ml were used as the calibrators. The sample peak area (R) versus drug concentration was analyzed by linear least square regression to obtain the equation of R = slope × concentration + y-intercept. The results, summarized in Table 4, show an excellent correlation between peak area ratio R and the concentration of the drug with $r^2 \geq 0.9999$.

Accuracy and precision were established by evaluating recoveries and R.S.D. values obtained with test solutions at concentrations of 0.05, 0.5, and 0.75 mg/ml. Within each set of validation experiments, three individual preparations were made at each concentration level. Recovery was calculated by comparing the theoretical concentration and the nominal concentration. The theoretical concentration was calculated from the calibration curve obtained within each set of validation experiment. The accuracy results (Table 5) showed recoveries between 99.4 and 101.1%. The intraday and intermediate precision values, as shown in Table 6, are less than 1.1 and 0.8% R.S.D., respectively.

The stability of SR16157 in the sample diluent, ACN/H_2O (1:1) with 0.1% TFA, is sufficient for the test solution to stay in the autosampler for 16 h during analysis, as is evident from the recoveries shown in Table 5, which were obtained from run sequences that lasted 16 h. The error due to decomposition was

Table 6
Precision: percent R.S.D. of three preparations/determinations at each concentration, and nine preparations/determinations at each concentration as the intermediate precision

	0.05 mg/ml	0.5 mg/ml	0.75 mg/ml
Validation 1	0.26	0.20	0.54
Validation 2	0.68	0.36	0.21
Validation 3	1.09	0.97	0.03
Intermediate	0.48	0.64	0.77

Table 7
Robustness

	t_R (min)	Number of theoretical plates	Resolution to component **a**	USP tailing factor
Flow rate (ml/min)				
0.9	14.6	11,122	1.60	1.52
1.0	13.4	9,905	1.56	1.49
1.1	12.0	9,869	1.52	1.44
Temperature (°C)				
23	13.5	10,081	1.87	1.48
27	13.4	9,905	1.56	1.49
31	12.7	11,597	1.19	1.78

less than 1%. Using a freshly prepared standard curve to assay a set of solutions (three preparations for each concentration, 0.05, 0.5, and 0.75 mg/ml) that were stored in the autosampler tray at room temperature for 24 h indicated a 2% decrease in the active drug, mainly due to hydrolysis of the drug to product **a**. It is recommended that the assay be performed within 16 h after the sample is dissolved in the diluent.

The robustness of the method was evaluated by analyzing a 0.5 mg/ml sample solution and evaluating performance parameters after varying, individually, the HPLC pump flow rate (±10%) and column compartment temperature (±4 °C). Results are presented in Table 7. Varying the flow rate did not cause significant changes in the following performance parameters of resolution (for SR16157 and component **a**), USP tailing factor and number of theoretical plates. Raising the column temperature to 31 °C, however, caused deterioration in resolution and an increase in the tailing factor.

The proposed assay method is of high sensitivity. The limit of detection (LOD) and limit of quantitation (LOQ) were obtained by serial dilution of the 0.05 mg/ml standard solution until the resultant chromatogram provided the SR16157 peak at a defined signal to noise ratio (S/N). Based on three and ten times S/N, the LOD and LOQ were determined to be 1.0 and 3.3 μg/ml, respectively.

4. Conclusion

An HPLC assay method has been developed and validated for SR16157. The HPLC method separates SR16157 from its impurities and forced decomposition products. Identities of the impurities and decomposition products have been elucidated by LC/MS and LC/UV spectral data. Major decomposition pathways are hydrolysis of the sulfamate, hydroxylation, oxidation, and hydrolysis of the ethyl side chain. The assay has been validated to be accurate (recovery = 99.4–101.1%), linear ($r^2 \geq 0.9999$), precise (intraday R.S.D. ≤ 1.1%, intermediate R.S.D. ≤ 0.8%), and sensitive (LOD = 1 μg/ml).

Acknowledgements

This work was funded by the Developmental Therapeutics Program, Division of Cancer Treatment and Diagnosis, National Cancer Institute, U.S. National Institutes of Health under Contract Nos. N02-CM-27134 and N02-CM-72203.

References

[1] J.R. Pasqualini, G.S. Chetrite, J. Steriod Biochem. Mol. Biol. 93 (2005) 221–236.
[2] R.J. Santen, D. Leszczynski, N. Tilson-Mallet, P.D. Feil, C. Wright, A. Manni, S.J. Santner, Ann. N.Y. Acad. Sci. 464 (1986) 126–137.
[3] S.J. Santner, P.D. Feil, R.J. Santen, J. Clin. Endocrinol. Metab. 59 (1984) 29–33.
[4] G.S. Chetrite, J. Cortes-Prieto, J.C. Philippe, F. Wright, J.R. Pasqualini, J. Steroid Biochem. Mol. Biol. 72 (2000) 23–27.
[5] T. Utsumi, N. Yoshimura, S. Takeuchi, M. Maruta, K. Maeda, N. Harada, J. Steroid Biochem. Mol. Biol. 72 (2000) 141–145.
[6] M.J. Reed, A. Purohit, L.W. Woo, S.P. Newman, B.V. Potter, Endocr. Rev. 26 (2005) 171–202.
[7] S.J. Stanway, P. Delavault, A. Purohit, L.W. Woo, C. Thurieau, B.V. Potter, M.J. Reed, Oncologist 12 (2007) 370–374.
[8] L. Rausch, A. Robb, P. Catz, S.E. LeValley, T. Harrison, K.L. Steinmetz, C.E. Green, J. Tomaszewski, K. Schweikart, N. Zaveri, J.C. Mirsalis, Proc. Am. Assoc. Cancer Res. 47 (2006) (Abstract # 3100).
[9] L.M. Rasmussen, N.T. Zaveri, J. Stenvang, R.H. Peters, A.E. Lykkesfeldt, Breast Cancer Res. Treatment. (2007) (Epub ahead of print).
[10] S. Görög, Anal. Sci. 20 (2004) 767–782.
[11] S. Görög, Fresenius Z. Anal. Chem. 309 (1981) 97–104.
[12] L. Nygaard, H.D. Kilde, S.G. Andersen, L. Henrisken, V. Overby, J. Pharm. Biomed. Anal. 34 (2004) 265–276.
[13] S.W. Baertschi, Trends Anal. Chem. 25 (2006) 758–767.
[14] L. Dorfman, Chem. Rev. 53 (1953) 47–144 (relevant data on page 96).
[15] S. Görög, B. Herényi, J. Chromatogr. 400 (1987) 177–186.
[16] A.E. Cribb, M.J. Knight, D. Dryer, J. Guernsey, K. Hender, M. Tesch, T.M. Saleh, Cancer Epidemiol. Biomarkers Prev. 15 (2006) 551–558.
[17] X. Xu, J.M. Roman, T.D. Veenstra, J. Van Anda, R.G. Ziegler, H.J. Issaq, Anal. Chem. 78 (2006) 1553–1558.
[18] J. Thibaudeau, J. Lepine, J. Tojcic, Y. Duguay, G. Pelletier, M. Plante, J. Brisson, B. Tetu, S. Jacob, L. Perusse, A. Belanger, C. Guillemette, Cancer Res. 66 (2006) 125–133.
[19] X. Xu, T.D. Veenstra, S.D. Fox, J.M. Roman, H.J. Issaq, R. Falk, J.E. Saavedra, L.K. Keefer, R.G. Ziegler, Anal. Chem. 77 (2005) 6646–6654.
[20] F. Modugno, K.E. Kip, B. Cochrane, L. Kuller, T.L. Klug, T.E. Rohan, R.T. Chlebowski, N. Lasser, M.L. Stefanick, Int. J. Cancer 118 (2006) 1292–1301.
[21] V. Rizzati, E. Rathahao, L. Gamet-Payrastre, G. Delous, I. Jouanin, F. Gueraud, A. Paris, Steroids 70 (2005) 161–172.
[22] G.M. Jacobsohn, M.K. Jacobsohn, Arch. Biochem. Biophys. 232 (1984) 189–196.